

Received April 7, 2019, accepted May 5, 2019, date of publication May 10, 2019, date of current version May 24, 2019.

Digital Object Identifier 10.1109/ACCESS.2019.2916029

# Experiments of Orbital Angular Momentum Phase Properties for Long-Distance Transmission

YU YAO<sup>ID</sup>, XIANLING LIANG<sup>ID</sup>, (Senior Member, IEEE), WEIREN ZHU<sup>ID</sup>, (Senior Member, IEEE), JUNPING GENG<sup>ID</sup>, (Senior Member, IEEE), AND RONGHONG JIN, (Fellow, IEEE)

Department of Electronics Engineering, Shanghai Jiao Tong University, Shanghai 200240, China

Corresponding author: Xianling Liang (liangxl@sjtu.edu.cn)

This work was supported by the National Natural Science Foundation under Grant 61571298, Grant 61671416, and Grant 61571289.

**ABSTRACT** In this paper, we propose a new method to effectively measure orbital angular momentum (OAM) properties for long-distance transmission. Properties of OAM wavefront in terms of phase and amplitude are measured by rotating the OAM wave antenna and fixing the plane wave antenna as a reference. To verify OAM phase properties for long-distance transmission, experiments are conducted in Tsingtao, China, with 3.7 km and 7.0 km across the Yellow Sea, which demonstrates that vortex phase properties of OAM keep well after long-distance transmission. Meanwhile, periodical properties of OAM waves' phase fronts are the same in different transmission distances.

**INDEX TERMS** Orbital angular momentum (OAM), rotation, long-distance transmission, vortex phase.

## I. INTRODUCTION

During the last decade, electromagnetic (EM) waves carrying orbital angular momentum (OAM,  $l$ ) has drawn considerable attentions at radio frequency due to infinitely orthogonal modes with OAM mode number  $l \in \mathbf{Z}$ . As a part of EM wave's angular momentum (AM), OAM is different from spin angular momentum (SAM,  $s$ ), which is associated with electromagnetic wave's polarizations with only three modes ( $s = 0, \pm 1$ ) [1]–[3]. OAM is related to helical phase front with vortex phase distribution  $e^{-jl\phi}$ , where  $\phi$  is the transverse azimuth angle of the EM wave. Meanwhile, there is null zone in the center of helical phase front due to the phase singularity of OAM. Before OAM is firstly proposed at radio frequency utilizing antenna array in 2007 [4], OAM properties has been analyzed at optical regime for several years [5]–[9]. Then, as a potential candidate of mode division multiplexing (MDM) at radio frequency, OAM properties with orthogonal modes can be applied to enhance transmission capacity in the communication system [10]–[13]. Because of abundant phase information, EM waves carrying OAM can also be seen as a potential candidate of radar detection system [14], [15].

EM waves carrying OAM at radio frequency can be achieved using constructed circular electric or magnetic sources with vortex phase distribution, such as phase plates [16], crafted antennas [17], metasurface [18] and antenna

arrays [19]–[21]. Using these generated OAM waves, experiments were conducted in laboratory environments or real environments to explore OAM properties applications [13], [22]–[24]. In existing published literatures, the longest OAM detection and application distance at radio frequency was conducted by Tamburini et al. in Venice with 442 meters distance [24]. On the other hand, due to null zones and vortex phase properties of OAM waves' helical phase fronts, EM waves carrying OAM are related to conical beams, whose beam peaks have divergence angles with respect to beam axes. The divergence effect can lead to the difficulty in receiving and utilizing OAM phase properties through a long-distance transmission. More seriously, how about OAM waves' vortex phase properties after long-distance transmission under the influence of divergence effect? Phase properties were only verified with short-distance transmission using the near field test system [25].

In this paper, phase and amplitude properties of OAM waves are analyzed and measured after long-distance transmission. The reminder of this paper is organized as follows. Section II presents the method and design of the experiment scheme exploring OAM wave front properties. Then, in Section III, the structure and performance of a multi-mode OAM antenna are presented, which is used as the transmitting OAM antenna. In Section IV, conducted experiments and corresponding experimental results in real environment are presented. Finally, Section V gives conclusions.

The associate editor coordinating the review of this manuscript and approving it for publication was Kai Lu.

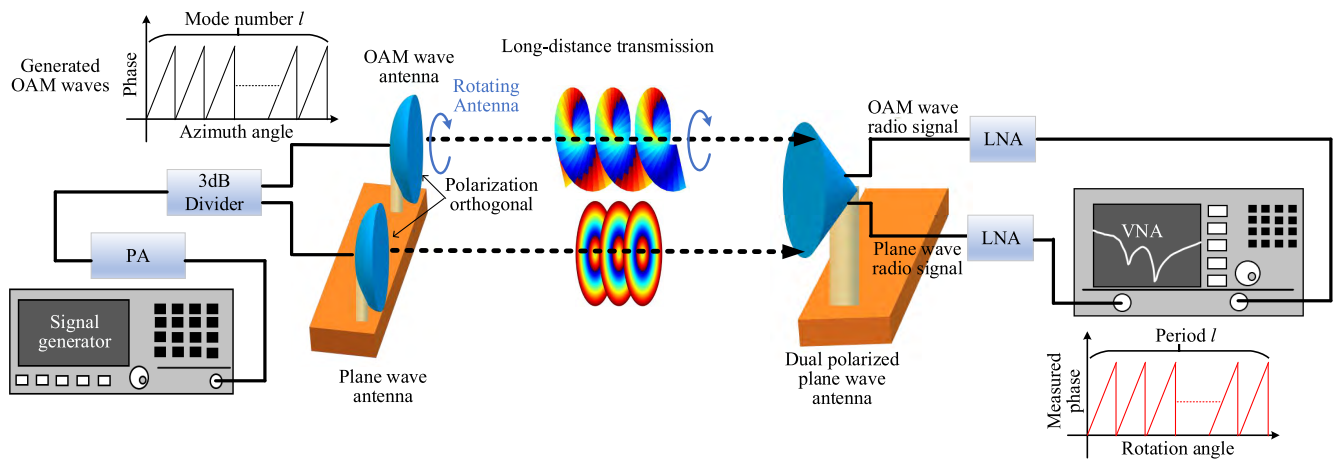


FIGURE 1. Scheme of the experiment exploring phase properties of EM waves carrying OAM for long-distance transmission.

## II. DESIGN OF THE EXPERIMENT

Scheme of the experiment presented in Fig. 1 is to explore phase properties for long-distance transmission. A closed test system is constructed to measure OAM vortex wave-front properties in the receiving antenna. It is noted that the conventional linked cables between transmitting and receiving antennas is unacceptable for long-distance transmission. Thus, in this paper, the plane wave is proposed as a reference signal to construct the long-distance closed test system measuring OAM wave phase properties. In order to separate the OAM wave and the plane wave effectively, these two waves employ two orthogonal polarizations. As shown in Fig. 1, the radio signal is generated by the signal generator and amplified using power amplifier (PA). Using a 3db power divider, the radio signal is divided into two parts. One part is transmitted into the OAM antenna with mode number  $l$  and another one is transmitted to the plane wave antenna. Generated OAM waves (mode number  $l$ ) have periodical properties with respect to the corresponding azimuth angle. After OAM wave propagating in the long distance, OAM wave and plane wave radio signals are both captured by the dual-polarized plane wave antenna with two low noise amplifiers (LNA). Utilizing receiver mode of vector network analyzer (VNA), phases and amplitudes of OAM waves can be measured and analyzed with respect to the plane wave radio signal.

Due to divergence effect of EM waves carrying OAM, cross section of complete vortex phase will get large along with transmission distance increasing. This divergence phenomenon leads to difficulty in capturing complete phase variation  $2l\pi$  in a period of azimuth angle shown in Fig. 1. Here, instead of changing receiving antenna's position with all azimuth angle  $\phi$ , rotating OAM wave antenna is applied. Correspondingly, phase fronts of OAM waves will rotate, complete phases and amplitudes properties of OAM wave-fronts' cross sections can be recorded, then mode number  $l$  can be revealed in a period of OAM antenna's rotation angle.

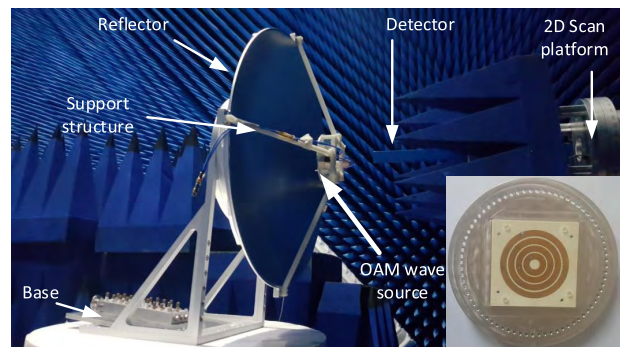
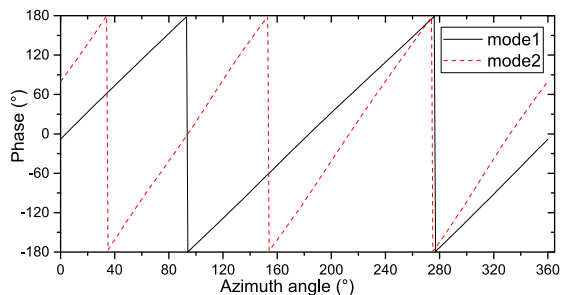


FIGURE 2. Structure of the OAM wave source on the parabolic reflector in the anechoic chamber.

## III. ANTENNA GENERATING OAM WAVES

As described in [26], [27], high order cavity mode  $TM_{(l|l+1)1}$  with  $90^\circ$  phase difference of the circular microstrip patch can be used to generate electromagnetic (EM) waves carrying OAM properties with mode number  $l$  and circular polarizations. Multi-concentric ring microstrip patches are applied to generate different OAM modes. Different ring microstrip patches are isolated from one another using metallic holes. Detailed parameters and analysis of the OAM wave source are shown in [28]. Utilizing external feeding networks, required orthogonal phases and same amplitudes of high order cavity mode  $TM_{(l|l+1)1}$  can be excited. However, due to the small gain and divergent beam generated by the multi-concentric ring microstrip patches, transmission distance of generated OAM beams are short. To alleviate divergence effect of OAM beams and enhance gain, the parabolic reflector is used and the multi-concentric ring microstrip antenna is used as its source. The OAM wave source is fixed on the focal point of the reflector with the plastic support structure, which is fabricated using 3D printing technology, and the reflector and the base are manufactured by aluminium alloy. Applying propagation properties of OAM analyzed in [25], focused OAM waves still have vortex properties. Using optimization



**FIGURE 3.** Simulated phase of LHCP OAM waves with mode number  $l = 1, 2$ .

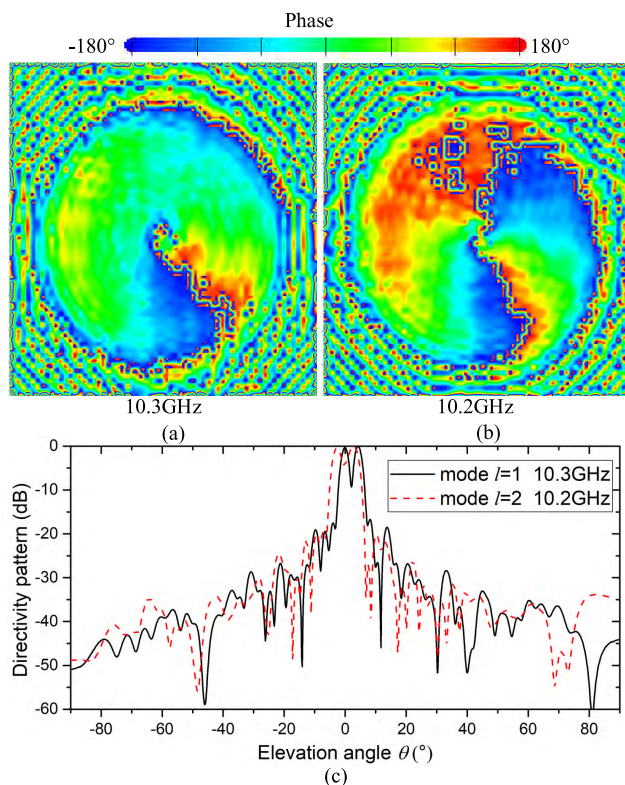


**FIGURE 4.** Measured results of LHCP EM waves generated by the reflector OAM antenna with mode number  $l = 1, 2$  at different frequencies: (a) x-polarized field's phase distribution of OAM mode number  $l = 1$  at frequency 10.3GHz (b) x-polarized field's phase distribution of OAM mode number  $l = 2$  at frequency 10.2GHz (c) cross sections of synthesized directivity pattern with mode number  $l = 1, 2$  at different frequencies.

of simulation software HFSS, optimized radius of the reflector is selected as 300mm and corresponding focal diameter ratio is chosen as 0.326 to focus energy of OAM wave as much as possible. Fig. 2 shows corresponding structure of the fabricated reflector OAM antenna. Simulated phase properties of generated left-hand circular polarization (LHCP) OAM waves with mode number  $l = 1, 2$  are shown in Fig.3 at peaks of gain. Phase variations have extra  $360^\circ$  phase variation compared to mode number. Circular polarization, which is also spin angular momentum (SAM) part of emitted OAM waves, leads to the phenomenon.

The field distribution of the fabricated reflector OAM antenna is measured using the near field test detector and

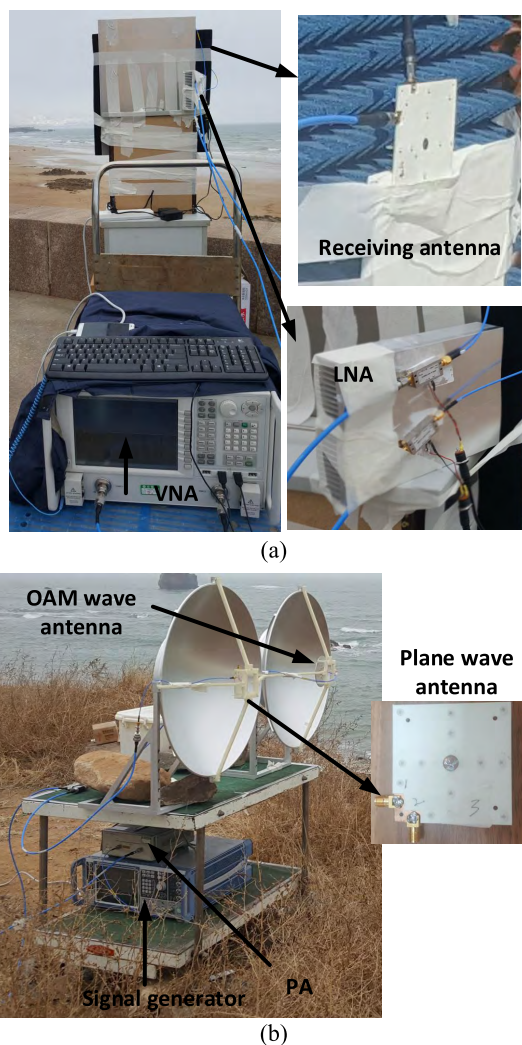


**FIGURE 5.** Placements of the transmitting antenna and receiving antenna in the experiment. (a) receiving antenna with VNA and LNA (b) transmitting antenna with PA and signal generator.

2D scan platform in the anechoic chamber. The near field test detector has linear polarization. Generated EM waves carrying OAM mode number  $l = 1, 2$  of the reflector OAM antenna are measured at frequency 10.3GHz and 10.2GHz, respectively. The reflector OAM antenna is 100mm away from the scanning plane. Meanwhile, scanning range of emitted EM waves is set as  $896\text{mm} \times 896\text{mm}$  with  $65 \times 65$  sampling points and the distance between adjacent sampling points is 14mm. All these distances are set to satisfy requirements of the near field scanning distance. Corresponding results of x-polarized fields' phase distributions and directivity patterns of OAM mode number  $l = 1, 2$  are both shown in Fig. 4. Phase distributions still have vortex properties of mode number  $l = 1, 2$ , especially near the center of the scanning plane. Using the near field test system, directivity pattern can also be synthesized as depicted in Fig. 4(c). Divergence angles of mode number  $l = 1, 2$  are respectively  $2.2^\circ$  and  $2.9^\circ$ , which are smaller than corresponding results of OAM wave source in [28]. Deviation angle of null zone



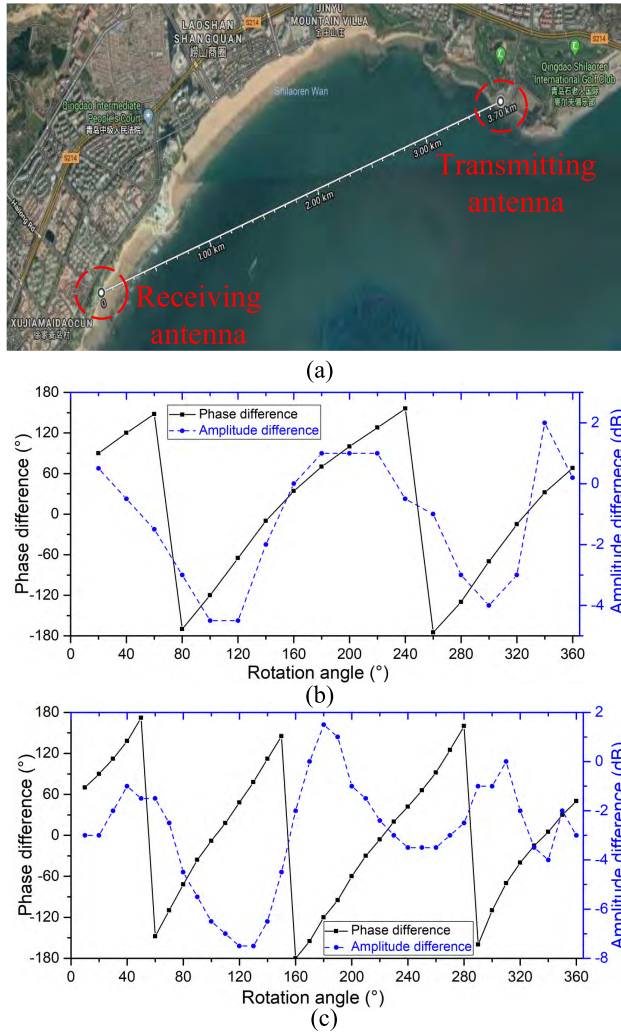


**FIGURE 6.** Experiment with 3.7km distance shown in the Google Earth and corresponding measured results of the experiment. (a) 3.7km experiment shown in Google Earth (b) measured phase and amplitude difference between OAM wave and plane wave with OAM mode number  $l = 1$  (c) measured phase and amplitude difference between OAM wave and plane wave with OAM mode number  $l = 2$ .

may be caused by misalignment of the near field test detector and the reflector OAM antenna. Overall, EM waves carrying OAM with mode number  $l = 1, 2$  and small divergence angle can be generated by the reflector OAM antenna. These waves are suitable for verifying OAM phase properties for long-distance transmission.

**IV. RESULTS AND DISCUSSIONS OF THE EXPERIMENT**

Experiments of OAM phase transmission properties in the long distance are conducted in Tsingtao, China. Placements of the transmitting antenna and receiving antenna in the experiment are both shown in Fig. 5. Using coaxial cables, the Agilent PA is connected to the signal generator Rohde&Schwarz SMF100A, which generates radio wave signal, meanwhile, the PA has the gain equalling to 30dB. The reflector OAM antenna has the polarization of LHCP and fixed right-hand circular polarization (RHCP) microstrip patch antenna is used to emit plane wave as the reference

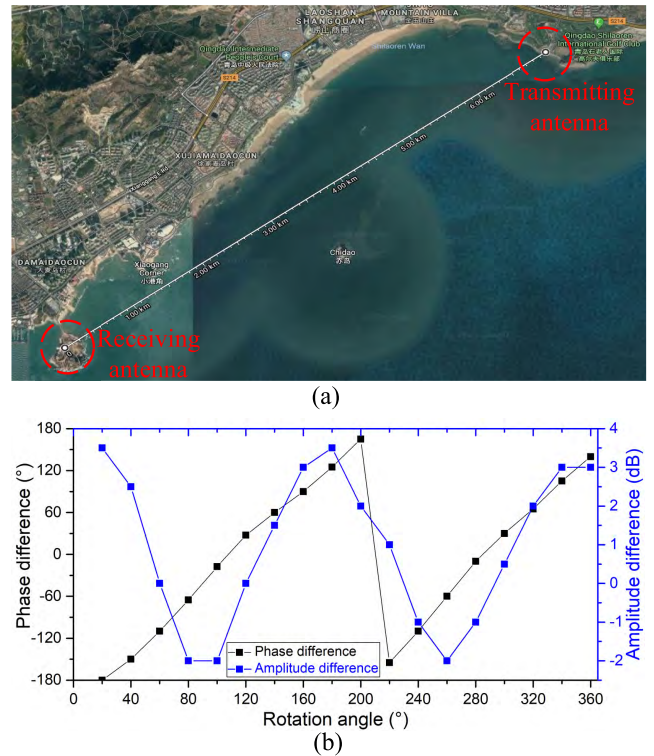


**FIGURE 7.** Experiment with 7.0km distance shown in the Google Earth and corresponding measured results of the experiment. (a) 7.0km experiment shown in Google Earth (b) measured phase and amplitude difference between OAM wave and plane wave with OAM mode number  $l = 1$ .

radio signal in the experiment. Moreover, in order to guarantee the capability of distinguishing background noise and reference radio signal, plane wave is also focused using the same parabolic reflector. At the receiving end, a dual-circular polarizations microstrip antenna is used to receive LHCP OAM wave's and RHCP plane wave's radio signals. In Fig.5(b), these orthogonal signals are separated into two coaxial cables and amplified using LNA. Gain of the LNA is 20dB. Using receiver mode of VNA, Agilent vector network analyzer E8361C is utilized to measure phase and amplitude differences between OAM wave radio signal and reference plane wave radio signal. After aligning both transmitting antenna and receiving antenna, rotating the OAM wave antenna around beam axis leads to the rotation of OAM wavefront at the receiving end. Utilizing the fixed RHCP plane wave signal as the reference radio signal, corresponding variation of phase and amplitude can be recorded, then OAM properties after long-distance transmission can be revealed.

As shown in Fig. 6(a), the experiment is conducted with 3.7km distance across the Yellow Sea. Signal generator's powers are 10dBm and 15dBm of mode number  $l = 1, 2$  separately. Corresponding variation of phase and amplitude difference are also recorded in Fig. 6(b)(c) with OAM mode number  $l = 1, 2$ . Received power of  $l = 1, 2$  reference plane waves are adjusted to  $-53\text{dBm}$  and  $-60\text{dBm}$ , which are close to received OAM waves' energies. With the increasing of OAM antenna's rotation angle, measured phases



of OAM radio signal change through 2 and 3 periods of  $360^\circ$  about mode number  $l = 1$  and 2, respectively. These phases' changes are caused by vortex phase properties of emitted OAM waves and corresponding results are accord with phase properties in Fig. 3. Compared to measured phase in Fig. 4(a,b), the phase variation has one extra  $360^\circ$  phase variation because of circular polarization. Mismatching tolerance, block of the support structure and the choppy sea may be the reason why amplitude difference in Fig. 6(b)(c) has fluctuation along with rotation angle increasing.

Furthermore, the distance of the experiment is increased to 7.0km, as depicted in Fig. 7. Generated power of signal generator is 15dBm and received power of plane wave is  $-57$ dBm. Position of receiving antenna is changed when position of transmitting antenna is fixed. In Fig. 7, corresponding phase still have periodical properties along with rotation angle increasing and these properties accord with vortex properties in Fig. 6(b). Thus, despite of the amplitude's fluctuation, vortex phase properties still exist after long-distance transmission and vortex phase fronts have same periodical phase transmission properties in different transmission distances.

## V. CONCLUSION

In this letter, experiments of OAM phase properties for long-distance transmission are presented. Scheme of the experiment is designed and analyzed. To construct the closed test system, the plane wave radio signal is used as the reference, which can also avoid utilization of long and heavy linked cables. For the long distance transmission, rotation of the OAM wave source is proposed to avoid changing position of the receiving end. Meanwhile, EM waves carrying OAM with different OAM modes generated by the microstrip antenna is focused using parabolic reflector to alleviate divergence effect and enhance transmission distances. Finally, experiments are conducted and verified with different transmission distance in Tsingtao, China. The transmission distance is 3.7km and 7.0km across the Yellow Sea. Vortex phase properties of OAM still exist after long-distance transmission across the sea in spite of the amplitude's fluctuation. Periodical properties of phase front are the same in different distances. Our experiments and results may offer more options and possibilities to utilize OAM properties in the real environment, especially in long-distance transmission.

## REFERENCES

- [1] J. H. Poynting, "The wave motion of a revolving shaft, and a suggestion as to the angular momentum in a beam of circularly polarised light," *Proc. Royal Soc. London A*, vol. 82, no. 557, pp. 560–567, 1909.
- [2] R. A. Beth, "Mechanical detection and measurement of the angular momentum of light," *Phys. Rev.*, vol. 50, no. 2, pp. 115–125, 1936.
- [3] J. A. Stratton, *Electromagnetic Theory*. New York, NY, USA: McGraw-Hill, 1941.
- [4] B. Thidé *et al.*, "Utilization of photon orbital angular momentum in the low-frequency radio domain," *Phys. Rev. Lett.*, vol. 99, no. 8, Aug. 2007, Art. no. 087701.
- [5] L. Allen, M. W. Beijersbergen, R. J. C. Spreeuw, and J. P. Woerdman, "Orbital angular momentum of light and the transformation of Laguerre-Gaussian laser modes," *Phys. Rev. A, Gen. Phys.*, vol. 45, no. 11, p. 8185, Jun. 1992.
- [6] G. Gibson, J. Courtial, M. J. Padgett, M. Vasnetsov, and V. Pas'ko, "Free-space information transfer using light beams carrying orbital angular momentum," *Opt. Express*, vol. 12, no. 22, pp. 5448–5456, 2004.
- [7] C. Paterson, "Atmospheric turbulence and orbital angular momentum of single photons for optical communication," *Phys. Rev. Lett.*, vol. 94, Apr. 2005, Art. no. 153901.
- [8] S. M. Barnett and L. Allen, "Orbital angular momentum and nonparaxial light beams," *Opt. Commun.*, vol. 110, nos. 5–6, pp. 670–678, 1994.
- [9] V. G. Fedoseyev, "Reflection of the light beam carrying orbital angular momentum from a lossy medium," *Phys. Lett. A*, vol. 372, no. 14, pp. 2527–2533, 2008.
- [10] X. Hui *et al.*, "Multiplexed millimeter wave communication with dual orbital angular momentum (OAM) mode antennas," *Sci. Rep.*, vol. 5, May 2015, Art. no. 10148.
- [11] J. Wang *et al.*, "Terabit free-space data transmission employing orbital angular momentum multiplexing," *Nature Photon.*, vol. 6, pp. 488–496, Jun. 2012.
- [12] X. Gao *et al.*, "An orbital angular momentum radio communication system optimized by intensity controlled masks effectively: Theoretical design and experimental verification," *Appl. Phys. Lett.*, vol. 105, no. 24, Dec. 2014, Art. no. 241109.
- [13] W. Zhang *et al.*, "Mode division multiplexing communication using microwave orbital angular momentum: An experimental study," *IEEE Trans. Wireless Commun.*, vol. 16, no. 2, pp. 1308–1318, Feb. 2017.
- [14] T. Yuan, H. Wang, Y. Qin, and Y. Cheng, "Electromagnetic vortex imaging using uniform concentric circular arrays," *IEEE Antennas Wireless Propag. Lett.*, vol. 15, pp. 1024–1027, 2016.
- [15] K. Liu, X. Li, Y. Cheng, Y. Gao, B. Fan, and Y. Jiang, "OAM-based multitarget detection: From theory to experiment," *IEEE Microw. Wireless Compon. Lett.*, vol. 27, no. 8, pp. 760–762, Aug. 2017.
- [16] S. Maccalli, G. Pisano, S. Colafrancesco, B. Maffei, M. W. R. Ng, and M. Gray, "q-plate for millimeter-wave orbital angular momentum manipulation," *Appl. Opt.*, vol. 52, no. 4, pp. 635–639, Feb. 2013.
- [17] F. Tamburini, E. Mari, and B. Thidé, C. Barbieri, and F. Romanato, "Experimental verification of photon angular momentum and vorticity with radio techniques," *Appl. Phys. Lett.*, vol. 99, no. 20, Nov. 2011, Art. no. 204102.
- [18] S. Yu, L. Li, G. Shi, C. Zhu, X. Zhou, and Y. Shi, "Design, fabrication, and measurement of reflective metasurface for orbital angular momentum vortex wave in radio frequency domain," *Appl. Phys. Lett.*, vol. 108, no. 12, Mar. 2016, Art. no. 121903.
- [19] S. M. Mohammadi *et al.*, "Orbital angular momentum in radio—A system study," *IEEE Trans. Antennas Propag.*, vol. 58, no. 2, pp. 565–572, Feb. 2010.
- [20] X.-D. Bai, X.-L. Liang, J. P. Li, K. Wang, J.-P. Geng, and R.-H. Jin, "Rotman lens-based circular array for generating five-mode OAM radio beams," *Sci. Rep.*, vol. 6, Jun. 2016, Art. no. 27815.
- [21] Y. Yao, X. Liang, W. Zhu, J. Geng, and R. Jin, "Phase mode analysis of radio beams carrying orbital angular momentum," *IEEE Antennas Wireless Propag. Lett.*, vol. 16, pp. 1127–1130, 2017.
- [22] Y. Ren *et al.*, "Line-of-sight millimeter-wave communications using orbital angular momentum multiplexing combined with conventional spatial multiplexing," *IEEE Trans. Wireless Commun.*, vol. 16, no. 5, pp. 3151–3161, May 2017.
- [23] M. Krenn *et al.*, "Twisted light communication through turbulent air across vienna," *New J. Phys.*, vol. 16, no. 11, Feb. 2014, Art. no. 113028.
- [24] F. Tamburini, E. Mari, A. Sponselli, B. Thidé, A. Bianchini, and F. Romanato, "Encoding many channels on the same frequency through radio vorticity: First experimental test," *New J. Phys.*, vol. 14, no. 3, Mar. 2012, Art. no. 033001.
- [25] Y. Yao, X. Liang, M. Zhu, W. Zhu, J. Geng, and R. Jin, "Analysis and experiments on reflection and refraction of orbital angular momentum waves," *IEEE Trans. Antennas Propag.*, vol. 67, no. 4, pp. 2085–2094, Apr. 2019.
- [26] M. Barbuto, F. Trotta, F. Bilotti, and A. Toscano, "Circular polarized patch antenna generating orbital angular momentum," *Prog. Electromagn. Res.*, vol. 148, pp. 23–30, May 2014.
- [27] Z. Zhang, S. Xiao, Y. Li, and B.-Z. Wang, "A circularly polarized multi-mode patch antenna for the generation of multiple orbital angular momentum modes," *IEEE Antennas Wireless Propag. Lett.*, vol. 16, pp. 521–524, 2017, doi: 10.1109/LAWP.2016.2586975.
- [28] M. Zhu, X. L. Liang, Y. Yao, J. Geng, W. Zhu, and R. Jin, "Eight-mode OAM microstrip antenna based on multi-ring structure," *Chin. J. Radio Sci.*, vol. 33, no. 4, pp. 455–462, Aug. 2018.



**YU YAO** was born in Anhui, China, in 1992. He received the B.Sc. degree from the University of Electronic Science and Technology of China, Chengdu, China, in 2014. He is currently pursuing the Ph.D. degree with Shanghai Jiao Tong University, Shanghai, China, under the supervision of Prof. R. Jin.

His current research interests include generation and propagation of orbital angular momentum waves.



**XIANLING LIANG** (M'11–SM'17) received the B.S. degree in electronic engineering from Xidian University, Xi'an, China, in 2002, and the Ph.D. degree in electric engineering from Shanghai University, Shanghai, China, in 2007.

From 2007 to 2008, he was a Postdoctoral Research Fellow with the Institute National de la Recherche Scientifique, University of Quebec, Montreal, QC, Canada. In 2008, he joined the Department of Electronic Engineering, Shanghai

Jiao Tong University (SJTU), Shanghai, as a Lecturer, and then became an Associate Professor, in 2012. He has authored or coauthored over 250 papers, including 141 journal papers and 113 conference papers, and coauthored one book and three chapters, in microwave and antenna fields. He holds 15 patents in antenna and wireless technologies. His current research interests include OAM-EM wave propagation and antenna design, time-modulated/4-D array and applications, anti-interference antenna and array, integrated active antenna and array, and ultra-wideband wide-angle scanning phased array.

Dr. Liang was a recipient of the Award of Shanghai Municipal Excellent Doctoral Dissertation, in 2008, the Nomination of the National Excellent Doctoral Dissertation, in 2009, the Best Paper Award from the International Workshop on Antenna Technology: Small Antennas, Innovative Structures, and Materials, in 2010, the SMC Excellent Young Faculty and the Excellent Teacher Award from SJTU, in 2012, the Shanghai Natural Science Award, in 2013, the Best Paper Award from the IEEE International Symposium on Microwave, Antenna, Propagation, and EMC Technologies, in 2015, the 4th China Publishing Government Book Award, and the Okawa Foundation Research Grant, in 2017.



**WEIREN ZHU** (M'16–SM'18) received the B.S. and Ph.D. degrees in physics from Northwestern Polytechnical University, Xi'an, China, in 2006 and 2011, respectively.

From 2011 to 2012, he was a Postdoctoral Fellow with the Nonlinear Physics Centre, Australian National University, Canberra, ACT, Australia. From 2012 to 2016, he was a Research Fellow with the Advanced Computing and Simulation Laboratory (A $\chi$ L), Department of Electrical and Computer

Systems Engineering, Monash University, Clayton, VIC, Australia. Since 2016, he has been with the Department of Electronic Engineering, Shanghai Jiao Tong University, Shanghai, China, as an Associate Professor. He has authored and coauthored over 100 refereed journal papers and over 40 conference proceedings. His current research interests include electromagnetic metamaterials, antennas and RF devices, and surface plasmon polaritons.

Dr. Zhu is a Senior Member of the Optical Society of America (OSA). He was a recipient of Shanghai Pujiang Talent Program by Shanghai Science and Technology Commission, in 2017. He is currently serving as an Associate Editor of the IEEE PHOTONICS JOURNAL and the IEEE ACCESS, and a Guest Editor of *Journal of Physics: Condensed Matter*.



**JUNPING GENG** (M'08–SM'17) received the B.S. degree in plastic working of metals, the M.S. degree in corrosion and protection of equipment, and the Ph.D. degree in circuit and system from Northwestern Polytechnic University, Xi'an, China, in 1996, 1999, and 2003, respectively.

From 2003 to 2005, he was a Postdoctoral Researcher with Shanghai Jiao Tong University. In 2005, he joined the faculty of the Electronic Engineering Department, Shanghai Jiao Tong University,

where he is currently an Associate Professor. From 2010 to 2011, he was a Visiting Scholar with the Institute Electrical and Computer Engineering, University of Arizona, Tucson, AZ, USA. He has authored or coauthored over 300 refereed journal and conference papers, three book chapters, and one book. He holds over 60 patents with over 40 pending. He has been involved with multiantennas for terminals, smart antennas, and nanoantennas. His main research interests include antennas, electromagnetic theory, computational techniques of electromagnetic, and nanoantennas.

Dr. Geng is a member of the Chinese Institute of Electronics (CIE). He was a recipient of the Technology Innovation Award from the Chinese Ministry of Education, in 2007, and the Technology Innovation Award from the Chinese Government, in 2008.



**RONGHONG JIN** (M'09–SM'13–F'17) received the B.S. degree in electronic engineering, the M.S. degree in electromagnetic and microwave technology, and the Ph.D. degree in communication and electronic systems from Shanghai Jiao Tong University (SJTU), Shanghai, China, in 1983, 1986, and 1993, respectively.

In 1986, he joined the Department of Electronic Engineering, SJTU, where he was an Assistant, a Lecturer, an Associate Professor, and is currently

a Professor. From 1997 to 1999, he was a Visiting Scholar with the Department of Electrical and Electronic Engineering, Tokyo Institute of Technology, Meguro, Japan. From 2001 to 2002, he was a Special Invited Research Fellow with the Communication Research Laboratory, Tokyo, Japan. From 2006 to 2009, he was a Guest Professor with the University of Wollongong, Wollongong, NSW, Australia. He is also a Distinguish Guest Scientist with the Commonwealth Scientific and Industrial Research Organization, Sydney, NSW, Australia. He has authored and coauthored over 400 papers in refereed journals and conference proceedings, and coauthored seven books. He holds more than 70 patents in antenna and wireless technologies. His current research interests include antennas, electromagnetic theory, numerical techniques of solving field problems, and wireless communications.

Dr. Jin is a Committee Member of the Antenna Branch of the Chinese Institute of Electronics, Beijing, China. He was a recipient of the National Technology Innovation Award, the National Nature Science Award, the 2012 Nomination of National Excellent Doctoral Dissertation (Supervisor), the 2017 Excellent Doctoral Dissertation (Supervisor) of the China Institute of Communications, the Shanghai Nature Science Award, and the Shanghai Science and Technology Progress Award.

...